

Metabolomic adjustments in the orchid mycorrhizal fungus *Tulasnella calospora* during symbiosis with *Serapias vomeracea*

Andrea Ghirardo^{1*} , Valeria Fochi^{2,3*} , Birgit Lange¹ , Michael Witting⁴ , Jörg-Peter Schnitzler¹ ,
Silvia Perotto^{2,3}  and Raffaella Balestrini³ 

¹Research Unit Environmental Simulation (EUS), Institute of Biochemical Plant Pathology, Helmholtz Zentrum München, Ingolstädter Landstr. 1, Neuherberg 85764, Germany; ²Department of Life Sciences and Systems Biology, University of Turin, Viale Mattioli 25, Torino 10125, Italy; ³Institute for Sustainable Plant Protection, National Research Council, Viale Mattioli 25, Torino 10125, Italy; ⁴Research Unit Analytical BioGeoChemistry, Helmholtz Zentrum München, Ingolstädter Landstr. 1, Neuherberg 85764, Germany

Summary

Authors for correspondence:

Raffaella Balestrini

Tel: +39 011 6502927

Email: raffaella.balestrini@ipsp.cnr.it

Silvia Perotto

Tel: +39 011 6705987

Email: silvia.perotto@unito.it

Received: 5 June 2020

Accepted: 6 July 2020

New Phytologist (2020)

doi: 10.1111/nph.16812

Key words: metabolomics, orchid mycorrhiza, *Serapias*, symbiosis, transcriptomics, *Tulasnella calospora*.

- All orchids rely on mycorrhizal fungi for organic carbon, at least during early development. In fact, orchid seed germination leads to the formation of a protocorm, a heterotrophic postembryonic structure colonized by intracellular fungal coils, thought to be the site of nutrient transfer. The molecular mechanisms underlying mycorrhizal interactions and metabolic changes induced by this symbiosis in both partners remain mostly unknown.
- We studied plant–fungus interactions in the mycorrhizal association between the Mediterranean orchid *Serapias vomeracea* and the basidiomycete *Tulasnella calospora* using nontargeted metabolomics. Plant and fungal metabolomes obtained from symbiotic structures were compared with those obtained under asymbiotic conditions.
- Symbiosis induced substantial metabolomic alterations in both partners. In particular, structural and signaling lipid compounds increased markedly in the external fungal mycelium growing near the symbiotic protocorms, whereas chito-oligosaccharides were identified uniquely in symbiotic protocorms.
- This work represents the first description of metabolic changes occurring in orchid mycorrhiza. These results – combined with previous transcriptomic data – provide novel insights on the mechanisms underlying the orchid mycorrhizal association and open intriguing questions on the role of fungal lipids in this symbiosis.

Introduction

In nature, most land plants associate with symbiotic fungi to form mycorrhizas. Depending on the morphology of the association and the taxonomic position of the symbiotic partners, four major mycorrhizal types are formed, namely arbuscular, ecto-, ericoid and orchid mycorrhizas (van der Heijden *et al.*, 2015). Mycorrhizal fungi increase the host plant's ability to acquire mineral nutrients and to tolerate biotic and abiotic stresses. In exchange, the fungal partner receives photosynthesis-derived carbon (C) as an energy source and takes advantage of a protected niche (Smith & Read, 2008). Orchids are peculiar because their minute seeds lack an endosperm and the symbiotic fungus provides the germinating seed and developing embryo with organic C, a strategy termed mycoheterotrophy (Leake, 1994; Merckx, 2013), as well as other nutrients such as N and P (Cameron *et al.*, 2006, 2007, 2008; Dearnaley & Cameron, 2017). Symbiotic seed germination leads to the formation of a small spherical body referred to as protocorm (Rasmussen, 1995), in which intracellular hyphal coils (or 'pelotons') are formed and are

thought to be responsible for nutrient transfer from the fungus to the host plant (Peterson & Farquhar, 1994).

Recently, the molecular bases underlying plant–microbe interactions in orchid mycorrhiza (OM) have been investigated (Yeh *et al.*, 2019). Gene expression profiling has identified fungal and plant genes putatively involved in signaling, symbiotic seed germination, mycoheterotrophy and plant defense (Zhao *et al.*, 2013; Perotto *et al.*, 2014; Kohler *et al.*, 2015b; Miura *et al.*, 2018; Lallemand *et al.*, 2019). Additionally, labeling experiments with stable isotopes (Cameron *et al.*, 2008; Kuga *et al.*, 2014) and molecular analyses (Zhao *et al.*, 2013; Fochi *et al.*, 2017a) have focused on nutrient exchanges between the symbionts.

Metabolomics is an alternative approach to the investigation of metabolic changes in symbiosis. Through the determination of the low-molecular-weight complement of biological systems (Kluger *et al.*, 2015), metabolomics provides direct information on the biochemical status of cells. Although little is known about metabolite alterations in OM, some plant secondary metabolites may play a role in the interaction. For example, the amount of lusianthrin, an antifungal stilbenoid initially identified in the orchid *Lusia indivisa* (Majumder & Lahiri, 1990), was increased in mycorrhizal protocorm-like bodies of *Cypripedium*

*These authors contributed equally to this work.

macranthos, suggesting a role in fungal control (Shimura *et al.*, 2007). Similarly, symbiotic *Anacamptis morio* protocorms were enriched in the phytoalexin orchinol, compared to nonmycorrhizal protocorms (Beyrle *et al.*, 1995). Some flavonoids, polyphenols, ascorbic acids and polysaccharides also increased in mycorrhizal orchids, compared to non-mycorrhizal plants (Chang & Chou, 2007).

Nontargeted metabolomics aims to investigate the entire metabolome, thus representing a powerful tool to profile thousands of metabolites potentially linked to nutrition and regulation of plant–fungal interactions, especially in combination with pathway analyses (Fiehn *et al.*, 2000; Aharoni *et al.*, 2002; Schlieemann *et al.*, 2008). It has previously been used to investigate plant–microbe interactions in legume root nodules (Zhang *et al.*, 2012), in roots colonized by the fungal endophyte *Piriformospora indica* (Hua *et al.*, 2017), in ectomycorrhizas (Tschaplinski *et al.*, 2014) and arbuscular mycorrhizas (Schlieemann *et al.*, 2008; Laparre *et al.*, 2014; Rivero *et al.*, 2015, 2018; Hill *et al.*, 2018).

Here, we employed metabolomics to investigate *in vitro* the mycorrhizal association between the Mediterranean orchid *Serapias vomeracea* and the basidiomycete *Tulasnella calospora* (Cantharellales). *Serapias vomeracea* seeds and *T. calospora* mycelium were grown together to form mycorrhizal orchid protocorms, and plant and fungal metabolite profiles were compared to those obtained when plant and fungus were cultivated separately as asymbiotic protocorms and free-living mycelium. We integrated metabolomic analyses with genomic information available for *T. calospora* (Kohler *et al.*, 2015a) and our previously published transcriptomic data (Fochi *et al.*, 2017a). In addition to differences in the metabolite profiles of symbiotic and asymbiotic protocorms, the results revealed intriguing and unexpected differences in the lipid content of free-living and symbiotic *T. calospora* mycelium.

Materials and Methods

Biological materials

Free-living mycelium of *T. calospora* *Tulasnella calospora* (Boud.) (AL13 isolate) was originally isolated from mycorrhizal roots of the terrestrial orchid *Anacamptis laxiflora* (Lam.) R.M. Bateman, Pridgeon and M.W. Chase in Northern Italy (Girlanda *et al.*, 2011) and was grown on solid 2% malt extract agar (MEA) at 25°C for 20 d before use. Three plugs (6 mm diameter) of actively growing mycelium were transferred onto a sterilized cellophane membrane placed on top of oat agar (OA, 0.3% milled

oats, 1% agar; Fig. 1a,d) – the same as that used for symbiotic seed germination – in 11 cm Petri dishes (Schumann *et al.*, 2013). After 20 d at 25°C, the free-living mycelium (FLM) was collected to avoid depletion of the culture medium and to keep the same growth conditions used previously for the

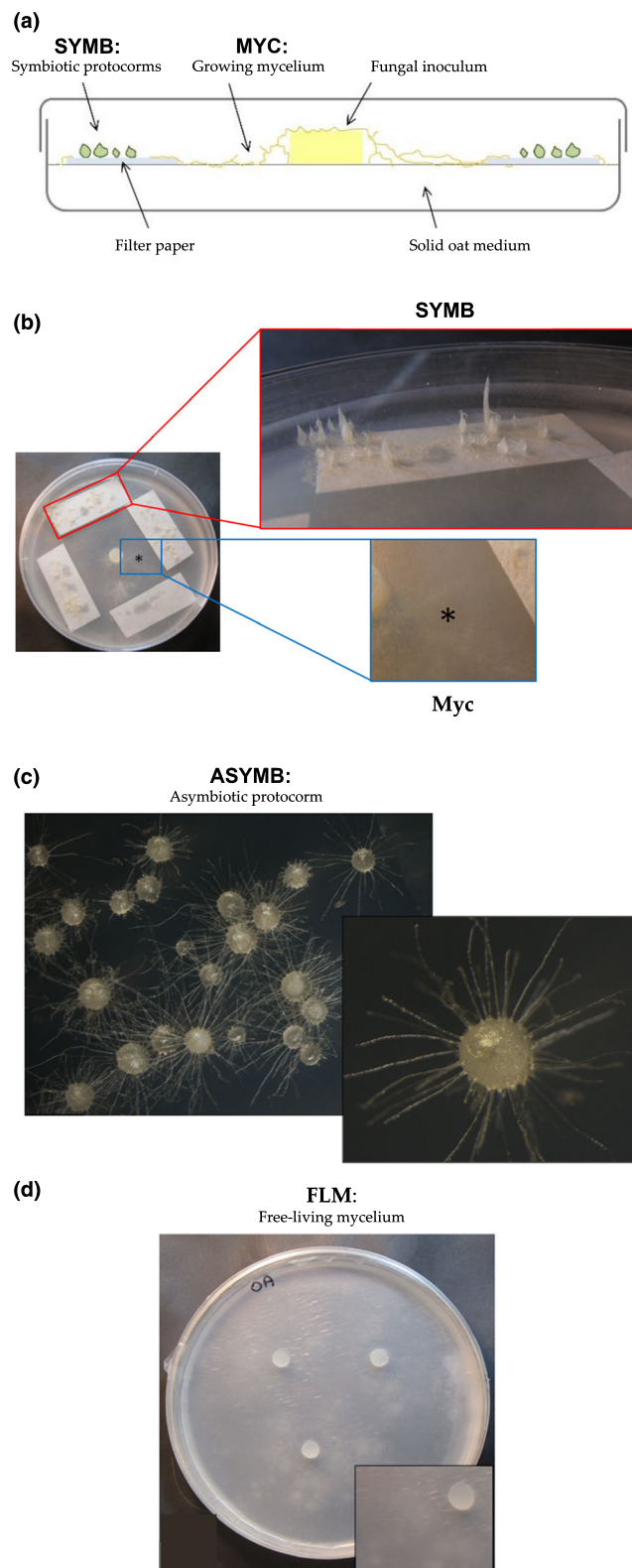


Fig. 1 (a) Schematic representation of the *in vitro* symbiotic germination system of *Serapias vomeracea* seeds with the orchid mycorrhizal fungus *Tulasnella calospora* (redrawn from Ercole *et al.*, 2015b). (b) Symbiotic seed germination in Petri dishes – mycorrhizal symbiotic protocorms (SYMB) of *S. vomeracea* (red box) and fungal mycelium (MYC) growing on a cellophane membrane near the symbiotic protocorms (blue box) after 30 d of co-incubation. (c) Asymbiotic protocorms (ASYMB) grown on BM1 medium 120 d after sowing. (d) Free-living mycelium (FLM) of *T. calospora* grown on a cellophane membrane on oat medium (OA) at 20 d post-inoculation (dpi).

transcriptomic analysis (Fochi *et al.*, 2017a), immediately frozen in liquid N₂ and stored at -80°C .

Symbiotic and asymbiotic germination of *S. vomeracea* seeds Symbiotic seed germination was obtained by co-inoculation of mycorrhizal fungus and orchid seeds in 9 cm Petri dishes (Ercole *et al.*, 2015). After surface sterilization, seeds were resuspended in sterile water and dropped on strips of autoclaved filter paper (1.5×3 cm) positioned on OA. A plug of actively growing *T. calospora* mycelium was then placed in the center of each Petri dish, and plates were incubated at 20°C in full darkness for 30 d in order to obtain healthy mycorrhizal protocorms (Fig. 1b), as previously reported (Fochi *et al.*, 2017a). Symbiotic germination was also performed by placing the mycelial plug on autoclaved cellophane membrane, in order to collect the fungal mycelium (MYC) growing near to the protocorms (Fig. 1c,d). Fungal mycelium samples were harvested by carefully scraping the mycelium with a spatula. Asymbiotic germination was achieved by placing surface-sterilized seeds directly on modified BM1 culture medium (Van Waes & Debergh, 1986) at 20°C in darkness. In order to have protocorms at the same developmental stage, symbiotic protocorms (SYMB) were collected at 30 d post-inoculation (dpi) and asymbiotic protocorms (ASYMB) at 120 dpi. All samples were flash-frozen in liquid N₂ and stored at -80°C .

Sample preparation for metabolomic analysis *Serapias vomeracea* symbiotic and asymbiotic protocorms and the *T. calospora* mycelium were disrupted with TissueLyser (18 Hz, 2 min, twice, Qiagen Diagnostic GmbH, Hilden, Germany). Frozen powder samples (100 mg) were extracted with 1 ml of methanol:isopropanol:water (1:1:1, v/v/v) for 1 h at 4°C with constant shaking. Subsequently, the solution was centrifuged at 18 620 g for 15 min at 4°C , and the supernatant was recovered, dried in a centrifugal evaporator (Savant SpeedVac, ThermoFisher Scientific, Bremen, Germany) and stored at -80°C . Before metabolomic analysis, the dried samples were dissolved in 200 μl of 50% acetonitrile in water and centrifuged at 18 620 g at 4°C for 10 min.

Ultra performance liquid chromatography ultra-high resolution tandem quadrupole/time-of-flight mass spectrometry (UPLC-UHR-QqToF-MS) measurements

Ultra performance liquid chromatography (UPLC) ultra-high resolution (UHR) tandem quadrupole/time-of-flight (QqToF) mass spectrometry (MS) measurements were performed on an Ultimate 3000RS (ThermoFisher, Bremen, Germany) coupled to a Bruker Impact II with Apollo II source (ESI source; Bruker Daltonic, Bremen, Germany). Chromatographic separation was achieved on a C₁₈ column (100×2.1 mm inner diameter with $1.7 \mu\text{m}$ particles; Fortis Technologies, Neston, UK). The eluents used were water with 0.1% formic acid (A), and acetonitrile with 0.1% formic acid (B). Gradient elution started with an isocratic hold of 0.5% B for 1 min, followed by an increase to 30% B in 15 min and a further increase to 80% B for 5 min. During the last 3 min, the initial conditions of 0.5% B were restored. The flow rate was $400 \mu\text{l min}^{-1}$ and the column temperature was kept at 40°C . The auto-sampler temperature was 4°C .

For each sample, two technical replicates were measured in both positive (+) and negative (−) ionization modes. Before sample analyses, quality control (QC) samples prepared from the aliquots of the different samples were injected for column conditioning. Mass calibration was achieved with 50 ml of water, 50 ml isopropanol, 1 ml sodium hydroxide, and 200 μl formic acid. The mass spectrometer was set up as follows: nebulizer pressure = 2 bar; dry gas flow = 10 l min^{-1} ; dry gas temperature = 220°C ; capillary voltage = 4000V for (+), 3000V for (−); endplate offset = 500V. Mass spectra were acquired in a mass range of 50–1300 m/z in both (\pm) modes.

Nontargeted metabolomic analysis

Each MS spectrum file was separately imported into the GENEDATA Expressionist for MS software v.13.5 (München, Germany) for peak picking and alignment. The pre-processing steps of the spectra in GENEDATA were: (1) chemical noise reduction, (2) retention time alignment, (3) identification of m/z features using the summed-peak-detection feature, (4) discarding of peaks not present in at least 10% of the mass spectra for isotope clustering, (5) discarding of singletons (clusters with only one member). The resulting peak matrix was exported, both (\pm) modes were combined, and the average peak intensity for both technical replicates was calculated and further used for statistical and annotation analyses. Peak intensities ranged between 0 and 4.6×10^6 . Mass features (m.f.) with positive values in less than three of the four biological replicates in one sample group and containing only zero values in other groups were removed from the data matrix. Finally, for the m.f. kept, zero values were set to 1. The resulting peak list was further used for annotation and statistical analysis. Metabolic annotation was achieved as previously described (Kersten *et al.*, 2013; Way *et al.*, 2013), using the portal MassTRIX3 (<http://masstrix3.helmholtzmuenchen.de/masstrix3>). Compared to MassTRIX (Suhre & Schmitt-Kopplin, 2008; Wägele *et al.*, 2012), the updated version, MassTRIX3, contains all metabolites of KEGG (<http://www.genome.jp/kegg/>), the Human Metabolome Database (HMDB – <http://www.hmdb.ca>), ChemSpider (<http://www.chemspider.com>), KNApSACk (<http://kanaya.naist.jp/KNApSACk>), Lipid Maps (<http://www.lipidmaps.org>) and PubChem (<https://pubchem.ncbi.nlm.nih.gov>). Putative molecular formulas were calculated from all m.f. using 4 ppm as a threshold. Molecular formulas were used to calculate H : C, O : C, N : C, P : C, S : C, and N : P ratios for the production of van Krevelen diagrams and for multidimensional stoichiometric compound classification (MSCC) (Rivas-Ubach *et al.*, 2018).

Pathway and functional analyses

Pathway analysis was performed using the Pathway Omics Dashboard tools of BioCyc (<https://biocyc.org/>; Paley *et al.*, 2017) on annotated metabolites, the concentrations of which changed significantly in MYC/FLM. We used METACYC v.23.1 (<https://metacyc.org>) as a reference database (Caspi *et al.*, 2018). The biological functions of the regulated annotated metabolites in MYC/FLM were obtained from the KEGG, HMDB and Lipid Maps databases.

Transcriptomic data

Symbiotic and asymbiotic growth conditions used for these metabolomic studies were the same as those previously investigated by transcriptomics in Fochi *et al.* (2017a). Transcriptomic data are, however, missing for the MYC samples. The complete series of fungal and plant transcripts are available at GEO (GSE86968 and GSE87120, respectively).

Statistical analysis

Experiments were performed using four independent biological replicates. Metabolomics data were analyzed by principal component analysis (PCA) and orthogonal partial least squares regression (OPLSR) (using SIMCA-P v.13; Umetrics, Umeå, Sweden). The pre-processing of the data followed established procedures (Ghirardo *et al.*, 2005, 2012, 2016). Discriminant masses (Kaling *et al.*, 2015) between the different mycelia (MYC and FLM) and the protocorms (SYMB and ASYMB) were further tested (*t*-test) for statistical significance using a false discovery rate (FDR) of 5% according to the Benjamini–Hochberg procedure (Benjamini & Hochberg, 1995) as previously described (Way *et al.*, 2013). Hypergeometric tests were performed using the function *phyper* in R v.3.6.0 (R Core Team, 2019).

Data availability

All UPLC-UHR-QqToF-MS raw data have been deposited in the open science framework data repository and are accessible at https://osf.io/5ayw7/?view_only=b315f2bf8fa9473cbe05417dd505ac33.

Results

Impact of symbiosis on plant and fungal metabolomes

The metabolome of symbiotic protocorms (SYMB) and *T. calospora* mycelium (MYC) collected near the symbiotic protocorms (Fig. 1a,b; Table 1) were compared with asymbiotic protocorms (ASYMB) and free-living mycelium (FLM) grown in pure culture on the same medium used for symbiotic seed germination

Table 1 Experimental growth conditions for untargeted metabolomics.

Sample ID	Experimental condition	Description
FLM	Free-living fungal mycelium on OA	Free-living mycelium of <i>Tulasnella calospora</i> grown on a complex OA medium
MYC	External fungal mycelium on OA	Mycelium of <i>T. calospora</i> grown on a complex OA medium and collected near <i>Serapias vomeracea</i> protocorms
SYMB	Symbiotic protocorms	<i>S. vomeracea</i> protocorms colonized by <i>T. calospora</i> on a complex OA medium
ASYMB	Asymbiotic protocorms	<i>S. vomeracea</i> protocorms grown on modified BM1 culture medium

OA, oatmeal agar medium.

(Fig. 1c,d; Table 1). We found a total of 24 818 metabolite-related mass features (m.f.), with the plant metabolomes being more complex (14 722 m.f. for SYMB, 16 213 for ASYMB) than the fungal metabolomes (4376 m.f. for MYC, 3337 for FLM).

The number of common and specific m.f. in symbiotic and asymbiotic plant samples and mycelia were visualized using a Venn diagram (Fig. 2). The 521 m.f. common to all samples are most likely related to a ‘core metabolome’ composed of primary metabolites found in both partners (Fig. 2). The 8583 m.f. that were found to overlap in SYMB and ASYMB samples, but were absent in MYC or FLM samples, likely represent plant metabolites involved in general plant functions of orchid protocorms. Several m.f. were unique to either symbiotic (SYMB, 3977) or asymbiotic (ASYMB, 5433) orchid protocorms. Although these unique m.f. could represent plant metabolites related to symbiosis, some may instead be the result of the different culture conditions required to grow symbiotic and asymbiotic protocorms at a similar developmental stage. For these reasons, a detailed comparison between SYMB/ASYMB samples was not considered, although it represented an important control for the identification of changes in the fungal partner. In particular, m.f. uniquely found in MYC, SYMB, and FLM samples (315) may be related to some fungus-specific compounds, as they were not found in ASYMB samples. Conversely, some m.f. (449) common to MYC, SYMB, ASYMB may be related to plant-specific compounds transferred from orchids to fungus. Of the unique 3977 m.f. found in symbiotic protocorms (SYMB), some may be related to symbiosis-specific metabolites from both mycorrhizal partners, that is, fungal compounds produced during protocorm colonization or fungal-induced plant compounds. Interestingly, a relatively high number of m.f. (1265) were uniquely found in MYC samples, indicating accumulation of distinct metabolites in the hyphae close to (but outside) the host plant. It is worth noting that none of the 291 and 315 m.f. uniquely found in MYC-

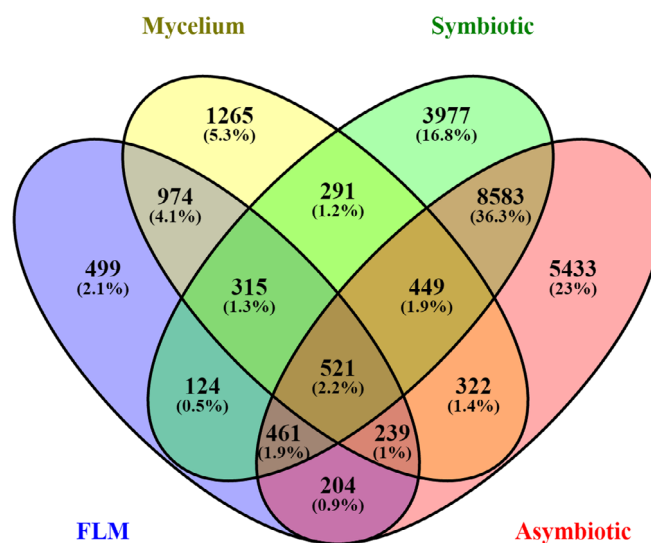


Fig. 2 Venn diagram of specific and shared mass features (m.f.) occurring and overlapping in symbiotic (SYMB) and asymbiotic (ASYMB) *Serapias vomeracea* protocorms, *Tulasnella calospora* free-living mycelium (FLM) and mycelium growing near symbiotic protocorms (MYC).

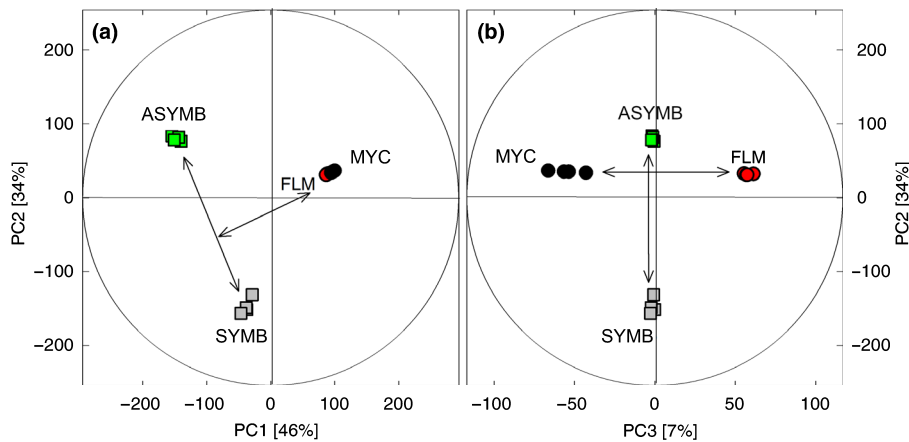


Fig. 3 Score plots of principal components analysis (PCA) for all mass features detected by nontargeted metabolomics. (a) Principal component (PC)1 vs PC2 shows the metabolic distances between *Tulasnella calospora* AL13 growing as free-living mycelium (FLM) or collected near the symbiotic protocorms (MYC), and between *Serapias vomeracea* symbiotic (SYMB) and asymbiotic (ASYMB) protocorms. (b) PC3 depicts metabolic differences between MYC and FLM. The variances explained by each PC are given in parentheses. Ellipses denote the Hotelling's T^2 confidence interval of 95%. $n = 4$ biologically independent replicates. ASYMB, green square; FLM, red circles; MYC, black circles; SYMB, grey square.

SYMB or in FLM-MYC-SYMB (Fig. 2) could be reasonably matched in databases; they likely represent symbiosis-specific compounds and constitutive fungal compounds, respectively.

In addition to unique and shared plant and fungal metabolites, the symbiotic plant–fungus interaction likely resulted in differential accumulation of a broader set of metabolites. Principal component analysis of all m.f. abundances comprehensively visualized changes in metabolite concentrations and showed a highly diverse metabolic profile among samples (Fig. 3). Not surprisingly, the most considerable distance (46%), as seen by the first component (PC1), was between ASYMB, SYMB and fungal mycelium (MYC/FLM). A further and significant distance among data was described by PC2 (34%), which clearly separated SYMB from ASYMB samples and, to a lesser extent, by PC3 (7%), MYC from FLM samples. Here, it must be noted that ASYMB contains a different growing medium, which likely contributes to the difference between ASYMB and the rest of the samples.

To gain insights into the metabolites and the metabolic pathways that are altered in symbiosis, we performed an OPLSR analysis followed by database annotation of the significant (adjusted $P < 0.05$, FDR 5%) discriminant masses (Kersten *et al.*, 2013). We putatively annotated the m.f. and calculated the \log_2 ratios of intensities (nondetected m.f. were set to 1) for SYMB/ASYMB, SYMB/MYC, SYMB/FLM, and MYC/FLM to assess metabolic regulation (see Supporting Information Table S1). Additionally, we employed the very recently developed MSCC approach, which classifies sum formulas for lipids, protein-related molecules, amino sugars, carbohydrates, nucleotides, and oxyaromatics (or phytochemicals) based on their elemental compositions (Rivas-Ubach *et al.*, 2018). This method avoids the limitations of actual database coverage, especially for less described organisms. The global metabolic changes of the main compound categories from annotated and nonannotated metabolites significantly and differentially accumulated during plant–fungus symbiosis are visualized in MSCC and van Krevelen diagrams

(Fig. 4, S1). The MSCC analysis highlighted the higher number of lipids that were increased in MYC, compared to FLM samples ($P < 0.001$, hypergeometric test, Fig. 4a; Table S2). Such an increase in MYC can also be seen in the van Krevelen diagram ($H/C \geq 1.32$ and $O/C \leq 0.6$, Rivas-Ubach *et al.*, 2018; Fig. 4c). Conversely, amino sugars and protein-related (i.e. N-containing) compounds were decreased in the MYC/FLM comparison ($P < 0.001$, hypergeometric test; Fig. 4a; Table S2).

Metabolic changes in the *T. calospora* mycelium

Metabolic changes caused by symbiosis were clearly detected in the external hyphae of *T. calospora* (Fig. 4a) and represent an aspect of the interaction that has so far remained unexplored. We first used the Pathway Omics Dashboard tool of MetaCyc as unbiased analysis to visualize the overall significant metabolic changes observed in fungus during its symbiotic interaction with the plant and in relation to lipids. When compared to FLM, the MYC metabolome had significantly higher levels (adj- $P < 0.05$) of compounds involved in lipid biosynthesis, followed by cell structures, hormones, carbohydrates, or compounds involved in metabolic regulation (Fig. 5).

Since MetaCyc was unable to classify $\sim 70\%$ of the annotated metabolites, we additionally investigated the chemical taxonomy and functions of regulated metabolites using data from the literature or available databases. This in-depth analysis showed that several compounds related to cell-structure and signaling were increased in MYC (Fig. 6; Table S1). Compared to lipids, notable changes in several N-, O- and S-containing compounds were observed in the external mycelium of *T. calospora* (Fig. 6a). With respect to functions, symbiosis caused an overall increase in the amount of structural, signaling, and energy-related compounds in MYC, as compared to FLM, mainly related to lipids (Figs 5, 6b; Table S1). Among lipids (120 metabolites), glycerophospholipids (GP, 68), fatty acyls (FA, 14), and isoprenoids (prenol lipids, 13) were considerably increased in MYC or not

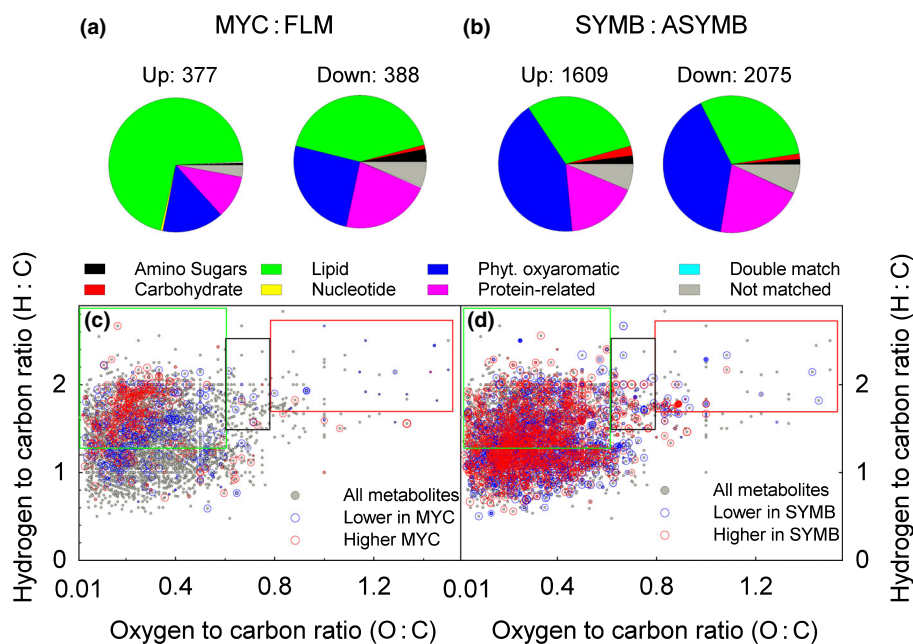


Fig. 4 (a, b) Multidimensional stoichiometric compound classification (MSCC) of significantly (adj. $P < 0.05$) differentially accumulated mass features (m.f.), and van Krevelen diagrams (c, d) showing all metabolites (in grey) and statistically increased (in red) or decreased (in blue) metabolites in asymbiotic and symbiotic conditions. ASYMB, asymbiotic orchid protocorms; FLM, asymbiotic free-living mycelium; MYC, fungal mycelium growing near the mycorrhizal protocorms; SYMB, symbiotic orchid protocorms. The magnitude of differentially accumulated metabolites are depicted in (c, d) with different symbol sizes (larger symbols represent stronger regulation), using $\sqrt{(\log_2(x))/2}$ for increased and $\sqrt{(-\log_2(x))/2}$ for decreased metabolites, where x is MYC/FLM (in c) or SYMB/ASYMB (in d). Rectangles in (c, d) indicate the limits for lipids (in green), amino sugars (in black) and carbohydrates (in red), according to Rivas-Ubach *et al.* (2018).

detected in FLM ($\log_2 > 10$) (Table S1). Among the few annotated metabolites from the 449 m.f. common to MYC-SYMB-ASYMB (Fig. 2) and significantly different in MYC/FLM, 32 were lipids, of which 15 were glycerolipids (GL) and 10 isoprenoids. Some N-containing organic compounds (29), organosulfur compounds (8), and oxy-aromatic metabolites (14) involved in defense were also highly increased in MYC. On the other hand, fewer lipids (48) (FA, 10; isoprenoids, 9), but more N-containing compounds (41), organosulfur compounds (17), and, among phytochemical compounds (17), alkaloids (14) were significantly decreased (Fig. 6).

The external mycelium of *T. calospora* showed specific changes in lipid content

The largest metabolomic differences between MYC and FLM were in the amount and composition of lipids (Figs. 6, S2; Table S1), in particular GP and sphingolipids (SP). Most of those metabolites were not detected in FLM, as seen in Table S1 for compounds with \log_2 values > 7.4 . Among the 81 GP that were increased in MYC, the compound with the largest value ($\log_2 = 21.4$) was putatively annotated as lysophosphatidylethanolamine (LysoPE), a lysophospholipid (LyP) involved in signaling. Notably, there was a considerable increase in the abundance of 18 glycerophosphoserines (GPS; $\log_2 > 10$) but a decrease in only one, and the abundance of the GP precursor palmitic acid was consistently increased ($\log_2 = 9.1$). Among GP, 13 phosphatidylcholines (PC) and 9 phosphoinositides (PI) were more abundant ($\log_2 > 10$) in MYC than in FLM. Also, a glycerophosphocholine, putatively annotated as 1-palmitoyl-sn-glycero-3-phosphocholine (LPC(16:0)) was increased ($\log_2 = 14.4$) in MYC samples. The GP phosphatidic acid PA (22:0/14:1(9Z)) – an essential intermediate in the biosynthesis of both triacylglycerols and GP, and therefore involved in energy (storage and source) and structural metabolism – also increased

($\log_2 = 12.9$) in MYC. The FA derivatives of hydroxyeicosatetraenoic acid, 15-HETE ($\log_2 = 21$), and 8-hydroxyoctadeca-9Z,12Z-dienoic acid (8-HODE or laetisarinic acid) ($\log_2 = 13.85$), an FA with allelochemical functions, were also highly increased in MYC. Moreover, the large accumulations of sphingosine ($\log_2 = 13.58$) and PI-Cer(d20:0/16:0) ($\log_2 = 12.58$) indicate an increase in SP biosynthesis in MYC.

Direct integration of metabolomic and transcriptomic data was unfortunately not possible because previous transcriptomic analyses (Perotto *et al.*, 2014; Fochi *et al.*, 2017a) did not investigate the MYC condition. However, significant changes in the expression of fungal genes involved in lipid metabolism (Table S3) were observed between SYMB and FLM. Among the fungal genes most upregulated in symbiosis (fold change, 'FC' > 10) were two members of the Ca^{2+} -independent phospholipase A_2 (Protein ID (#) 53822, #25657) and a myo-inositol-1-phosphate synthase (#72491), which are essential for the biosynthesis of inositol-containing phospholipids (PI) and certain SP signaling molecules. Two fungal genes corresponding to phosphoinositide kinases (FC = 4.6, #26793, FC = 2.4, #28485) and three sphingosine N-acyltransferases, a key enzyme involved in SP biosynthesis, were upregulated in symbiosis (#18228, #79587, #18227) (Table S3). Conversely, the abundance of one glucosylceramidase (#33445) decreased considerably. Several genes involved in FA metabolism through the Acyl-CoA coenzyme were also affected (Table S3), including two downregulated genes coding for thiolases (#16280, #131995).

Finally, we observed large changes of 29 isoprenoids in the MYC/FLM comparison (Table S1), with 10 being found in MYC-SYMB-ASYMB but not in FLM. In particular, eight triterpenoids, one diterpene and one tetraterpene were markedly increased ($\log_2 > 10$). Although transcriptional information on the MYC condition is not available, five *T. calospora* genes

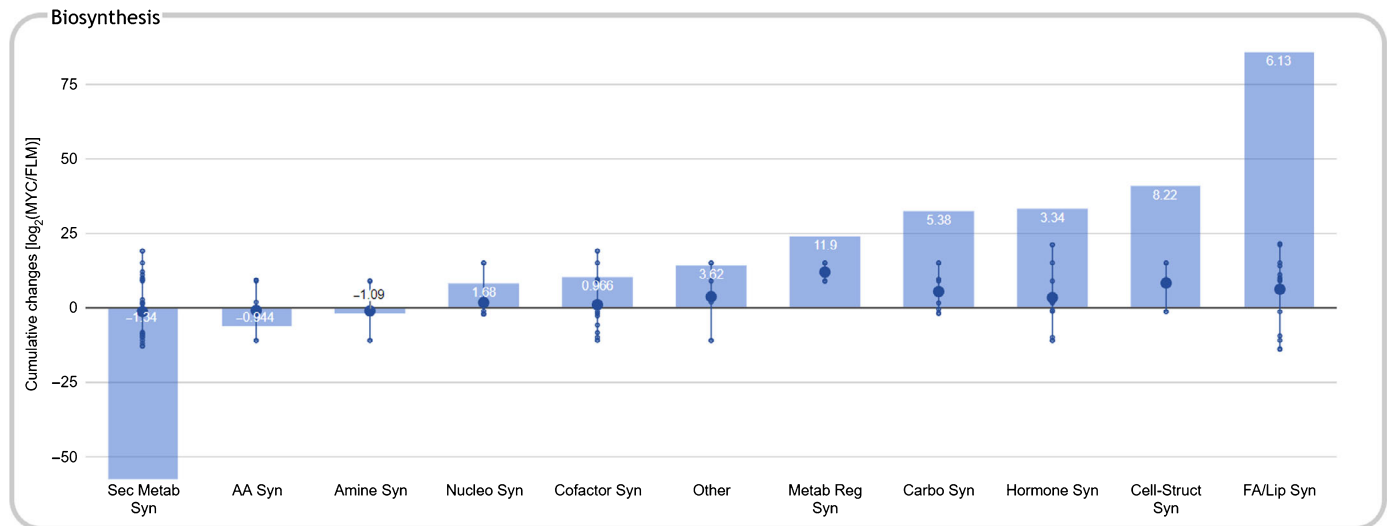


Fig. 5 Cumulative changes in significantly and differently produced compounds from the metabolism of MYC samples, compared to FLM. Each dot shown along a vertical line corresponds to the log₂ change ratio of MYC/FLM for a single metabolite. The large dot shown on each line is the average of all metabolites present for the metabolite class. FLM, asymbiotic free-living mycelium; MYC, fungal mycelium growing near the mycorrhizal protocorms. The functional classes are based on the MetaCyc pathway ontology (<https://metacyc.org/>) and the graph was constructed using the Omics Dashboard (Paley *et al.*, 2017).

encoding terpenoid synthases were significantly upregulated in symbiotic protocorms (Table S3), two of them with FC > 20 (#70959, #22905).

Nitrogen-containing fungal compounds Nitrogen-containing (nonphospholipid) compounds were the second group of metabolites significantly affected in *T. calospora*, with a large decrease in MYC, relative to FLM (Fig. 6a; Table S1). Although most of these compounds could not be reliably annotated, they indicate large changes in fungal N metabolism during symbiosis. Two of the few identified compounds with increased levels in MYC compared to FLM were UDP-N-acetyl-D-glucosamine (UDP-GlcNAc; log₂ = 9.52) and dolichyl-N-acetyl- α -D-glucosaminyl-phosphate (log₂ = 11.47), N-containing compounds that are essential for the biosynthesis of N-linked glycans, glycosylphosphatidylinositol (GPI)-anchored proteins, SP and glycolipids. UDP-N-acetyl-D-glucosamine can be polymerized to form chitin, a major component of fungal cell walls. Short oligomers of chitin and chitosan, its deacetylated form, were found to be similarly enriched (log₂ from 11.9 to 13.6) in SYMB compared with either MYC or FLM, whereas no differences were observed between MYC and FLM (Table S1). Chitosan is produced through the activity of chitin deacetylase, and three chitin deacetylase genes (#174258, #26855, #107589) out of the nine present in the *T. calospora* genome were significantly upregulated in SYMB with respect to FLM (Table S3). By contrast, a single chitin synthase (#31299) was slightly upregulated in symbiosis (FC = 2, Table S3). Short chitin oligomers could be also generated from long chitin polymers by chitinase activity. The expression of both fungal and plant chitinases was modified by symbiosis (Tables S3, S4), with some plant chitinases being strongly upregulated in symbiotic protocorms (TRINITY Contig

Names: DN77284_c0_g1_i3, DN5745_c0_g1_i1, DN66370_c0_g1_i1, DN62020_c0_g1_i1).

Comparing symbiotic and asymbiotic conditions, another primary class of regulated N-containing compounds was involved in amino acid (AA) metabolism (Table S1). Accumulation of N-L-argininosuccinate was found in SYMB when compared to all other samples (log₂ = 3.8 with ASYMB; log₂ = 13.3 with MYC and FLM). This compound is involved in arginine biosynthesis and fumarate formation, an essential intermediate of the TCA cycle. Unfortunately, the metabolomic study of symbiotic tissues (SYMB) is not easy, as they contain both plant and fungal metabolites, and assignment of most mass features to the symbionts is uncertain. Therefore, most AA and AA derivatives could not be assigned to the fungus or to the plant, with few exceptions. One was the putatively annotated ergothioneine, a naturally occurring metabolite of histidine exclusively found in some fungi and bacteria (Cumming *et al.*, 2018), which was only detected in SYMB. The concentrations of hercynine, another fungal-specific and histidine related compound, were, by contrast, low (log₂ = -10.31) in SYMB/MYC. Transcriptomic evidence points to an important role of *T. calospora* in histidine biosynthesis during symbiosis, with three biosynthetic genes (#108905, #73648, #141375) being significantly upregulated in SYMB samples (Table S3).

Organosulfur compounds Significant changes in S-containing compounds were observed in *T. calospora* (Table S1), with 14 compounds showing an increase (log₂ > 10) and 18 showing a decrease (log₂ < -10) in MYC, compared to FLM. Similar to N-containing compounds, many organosulfur compounds could not be reliably annotated. An exception was S-adenosylmethionine, a decarboxylated derivative of S-adenosylmethionine

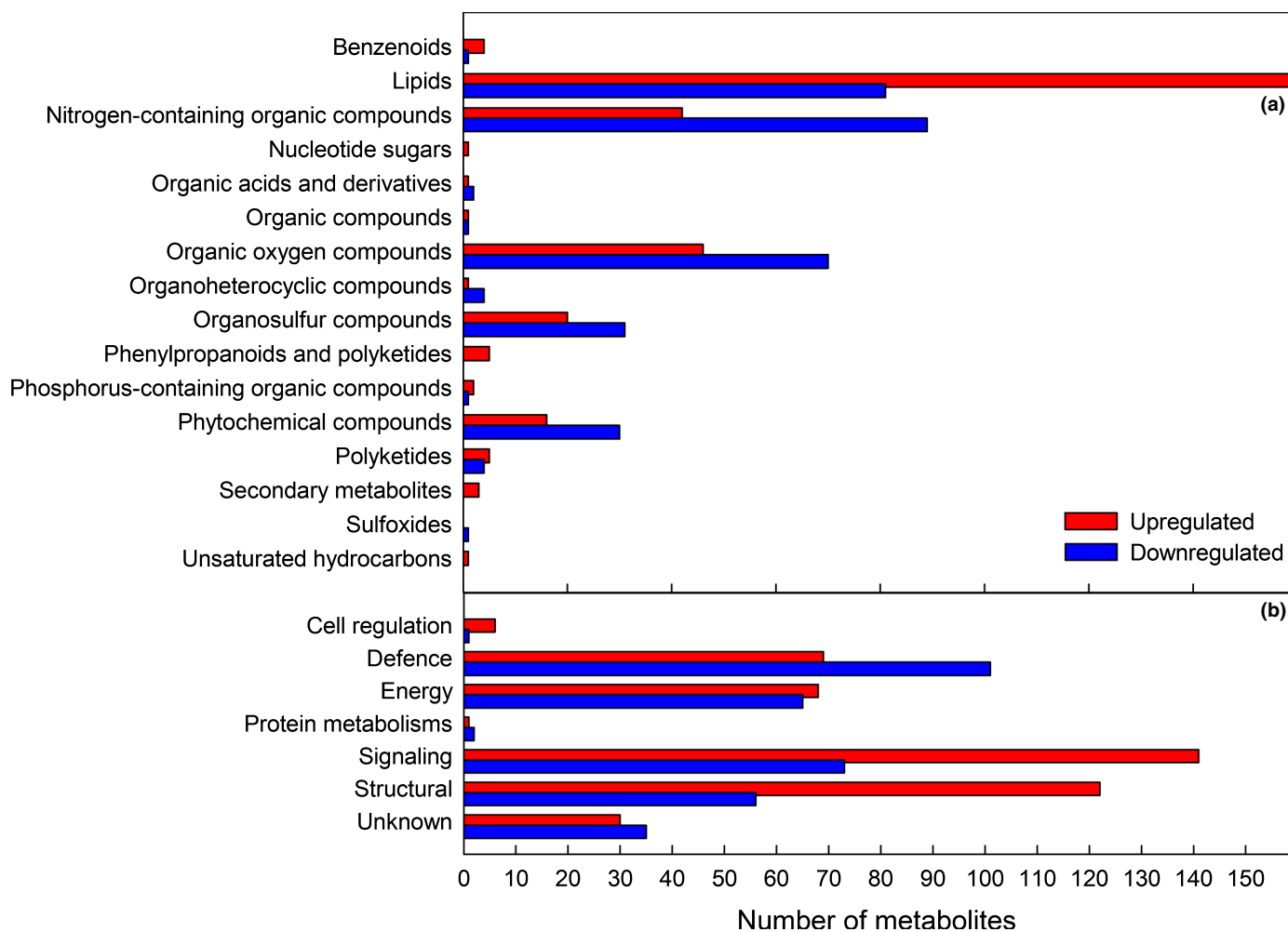


Fig. 6 Changes in metabolites in the *Tulasnella calospora* mycelium. The number of metabolites is shown, grouped according to (a) their chemical taxonomy and (b) the biological functions of the increased (in red) and decreased (in blue) metabolites in MYC samples, relative to FLM. A comprehensive list is given in Supporting Information Table S1. The classification is based on data from the KEGG, HMDB and Lipid Maps databases. Unknown organic compounds were classified based on the following priority of their atom compositions: S > P > N > O. For multifunction metabolites, the functions were added to different groups.

(SAM) that is involved in polyamine biosynthesis (Pegg *et al.*, 1998). Notably, the amount of S-adenosylmethionine in MYC was markedly reduced ($\log_2 = -11.05$) compared to FLM, whereas the amount of SAM was increased ($\log_2 = 8.9$). S-adenosylmethionine is a major source of methyl groups for reactions involving methylation. The substantial SAM accumulation in MYC (Table S1) suggests a role in symbiosis. Although SAM levels did not significantly differ in SYMB/MYC or SYMB/FLM (Table S1), transcriptomics revealed that the *T. calospora* SAM synthetase gene was upregulated (FC = 4.28, #72837) in symbiosis (Table S3). Metabolomic data further indicate a significantly lower ($\log_2 = -10.3$) SAM content in SYMB as compared to ASYMB (Table S1), suggesting a decrease in plant SAM in symbiosis.

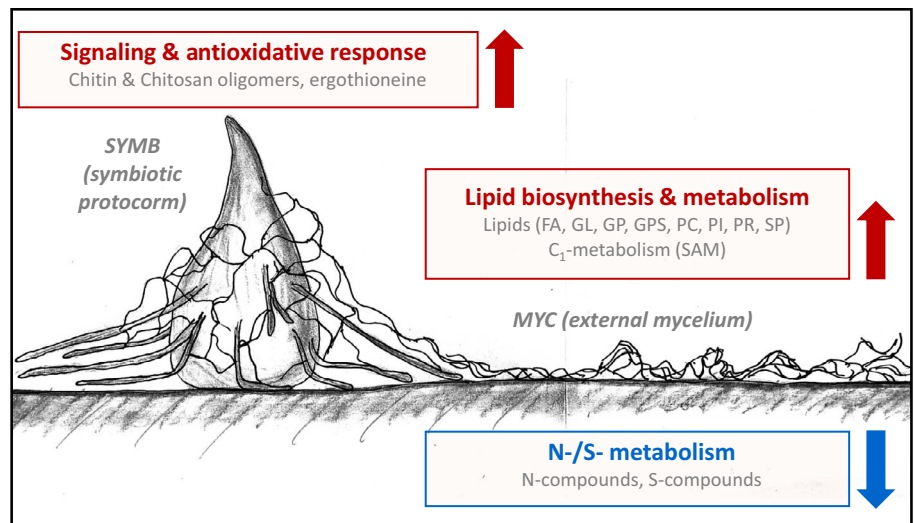
Discussion

Transcriptomics is the most common approach for indirect investigation of metabolic changes in symbiotic organisms

because it reveals the contributions of both partners through changes in their gene expression. This approach was successfully used on OM protocorms, where plant and fungal molecules are mixed and cannot be separated before analyses (Zhao *et al.*, 2013; Fochi *et al.*, 2017a; Miura *et al.*, 2018). However, transcriptional regulation of genes encoding enzymes does not necessarily reflect the final enzymatic activity, questioning the direct association between metabolites and transcripts (Cavill *et al.*, 2016). Therefore, we used a nontargeted approach to directly investigate metabolic changes in OM, using transcriptomic data to corroborate metabolomic results. The major findings are summarized in Fig. 7.

Comparison of the plant metabolomes was hampered by the different growth conditions and media needed to obtain SYMB and ASYMB protocorms at a similar developmental stage. However, metabolites from ASYMB protocorms allowed us to assess the contributions of plant and fungal products in the symbiosis. Metabolomics yielded particularly interesting results when the MYC mycelium was compared with the free-living mycelium.

Fig. 7 Schematic overview of fungal metabolic changes in symbiotic protocorms (SYMB) and in the mycelium surrounding and in contact with the protocorm (MYC), as compared to free-living *Tulasnella calospora* mycelium (FLM). FA, fatty acyls; GL, glycerolipids; GP, glycerophospholipids; GPS, glycerophosphoserines; PC, phosphatidylcholines; PI, phosphoinositides; PR, prenol lipids (syn. isoprenoids); SP, sphingolipids; SAM, S-adenosylmethionine.



Although we cannot exclude the possibility that the conditions required to grow symbiotic and asymbiotic fungal mycelia had some influence on the metabolite profile, the major changes of metabolite profiles seen in MYC were most likely driven by protocorms. Previous studies on ericoid mycorrhiza revealed that the symbiotic interaction is a major determinant of transcriptomic changes in the fungus, much larger than environmental growth conditions (Casarrubia *et al.*, 2020). In the OM symbiosis, all organic nutrients needed by the protocorms are thought to be provided by the fungus. Thus, most metabolites identified in MYC are likely produced by *T. calospora* and differentially accumulated in the presence of the plant, even if we cannot exclude the possibility that some plant-derived organic compounds may be transferred to the symbiotic fungus. Such plant compounds may be found among the mass features common to MYC, ASYMB and SYMB (449 mass features) or common to MYC and SYMB (219 mass features). Unfortunately, we could not confirm the plant or fungal origin of these compounds – this was also due to the lack of transcriptomic data under MYC conditions (Perotto *et al.*, 2014; Fochi *et al.*, 2017a).

Symbiosis caused profound changes in the lipid content of *T. calospora*

Lipids were the most prominent metabolites that were differentially accumulated in MYC, compared to FLM. Besides being major structural components of cell membranes, lipids provide critical biological functions as energy and carbon storage, in signaling, stress response and plant–microbe interactions (Siebers *et al.*, 2016). Lipids have recently become an important topic in mycorrhizal research because a substantial increase in the amount of lipids was discovered in the hyphae of arbuscular mycorrhizal fungi during symbiosis (Keymer *et al.*, 2017). Arbuscular mycorrhizal fungi are obligate biotrophs that cannot synthesize fatty acids, and lipids are transferred from the plant. By contrast, the *T. calospora* genome contains the genetic machinery for lipid biosynthesis, and although we cannot

exclude some lipid transfer from the plant, the increased lipid content in the external *T. calospora* hyphae more likely reflects endogenous biosynthesis.

Phospholipids and sphingolipids are vital components of cell membranes and play key roles in signaling, cytoskeletal rearrangement and membrane trafficking (Meijer & Munnik, 2003; Singh & Del Poeta, 2016; Hannun & Obeid, 2018; Blunsom & Cockcroft, 2020). In fungi, sphingolipids are important for hyphae formation (Oura & Kajiwara, 2010), regulating cell growth and differentiation (Obeid *et al.*, 2002), and cell division (Epstein *et al.*, 2012). In addition, lipid-derived molecules are essential for intra- and extra-cellular signaling and for defense against the proliferation of undesired microbes (Siebers *et al.*, 2016; Singh & Del Poeta, 2016; Wang *et al.*, 2020).

Overall, we observed a general increase in several structural lipid constituents of cell membranes and of their metabolic precursors (e.g. palmitic acid and UDP-GlcNAc). Palmitic acid is one of the most common saturated fatty acids found in animals, plants and microorganisms, and the first fatty acid produced during lipogenesis (Sidorov *et al.*, 2014; Carta *et al.*, 2017). UDP-N-acetyl-D-glucosamine, an essential precursor of chitin, is also involved in the biosynthesis of sphingolipids and sulfolipids (Bowman & Free, 2006; Ebert *et al.*, 2018). The lipids that were found to be most markedly increased in MYC were glycerophospholipids, in particular phosphatidylserine, which plays a role in the functioning of several intracellular signaling proteins and the activation of specific kinases (Kay & Grinstein, 2011). Sphingosine and PI-Cer(d20:0/16:0) are precursors of sphingolipids which are also important components of fungal cell membranes (Meijer & Munnik, 2003; Singh & Del Poeta, 2016). The abundances of these compounds as well as those of nine other phosphoinositides increased markedly in MYC, likely reflecting the upregulation in symbiosis of phosphoinositide phosphatases and serine/threonine protein kinases, key enzymes involved in the biosynthesis of sphingolipids and glycerophosphoinositols (Hannun & Obeid, 2018; Blunsom & Cockcroft, 2020).

Some membrane lipids play essential roles in pathogenic and mutualistic interactions. For example, changes in membrane lipid compositions of rhizobia, including phosphatidylserine and phosphatidylethanolamine, prevented the formation of N-fixing legume nodules (Vences-Guzmán *et al.*, 2008). In fungi, the same two lipid classes have been correlated with *Candida albicans* virulence (Cassilly & Reynolds, 2018), and an increase in phosphatidylserine was observed during fungal differentiation in the phytopathogenic *Rhizoctonia solani* (Hu *et al.*, 2017). Early intermediates of sphingolipids are also essential for normal appressoria development and pathogenicity in *Magnaporthe oryzae* (Liu *et al.*, 2019).

In addition to structural membrane components, we observed in MYC a strong increase in lipids involved in signaling and defense. Lysophospholipids in plants are essential signaling molecules and growth regulators (Meijer & Munnik, 2003; Cowan, 2006). The fatty acid 8-HODE (or laetisarinic acid) originates from linoleic acid and is a bioactive oxylipin acting as a signal in plant–fungus interactions (Brodhun & Feussner, 2011; Christensen & Kolomiets, 2011). 8-HODE was first discovered in the basidiomycete *Laetisaria arvalis* as an allelochemical that suppresses growth of phytopathogenic fungi (Bowers *et al.*, 1986). In MYC, the strong increase in 8-HODE and 15-HETE, a hydroxylated fatty acid substrate for oxylipin biosynthesis, indicates that the signaling apparatus in MYC is highly active during symbiosis. Interestingly, some Ca^{2+} independent phospholipases A_2 , which act in membrane homeostasis, signal transduction, and virulence (Valentín-Berríos *et al.*, 2009), were among the most upregulated *T. calospora* genes.

Although the increased abundance of structural membrane lipids in the external hyphae may simply reflect stimulation of hyphal growth and a need for membrane biogenesis following symbiosis, the increase in potential membrane signaling molecules is intriguing.

N- and S-containing organic compounds in the external *T. calospora* mycelium

Compared to lipids, the large decrease in the percentage of N- and S-containing compounds in the MYC samples is more difficult to explain (Figs 4, 6). In our system, the fungus likely provides the host with organic N, as suggested by the strong upregulation of some plant AA transporters in the mycorrhizal protocorm cells (Fochi *et al.*, 2017a,b). We could, therefore, speculate that depletion of some N-containing compounds in MYC may be the result of N-transfer to the host. It is also possible that some of the nonannotated compounds that exhibited increased abundances are simply involved in the metabolism of N-containing lipids or N-containing polysaccharides, such as chitin and derivatives (see paragraph below).

Regarding sulfur, there is currently no information on its transfer to the host plant in OM. Among the few S-containing compounds that could be reliably identified, SAM was increased in MYC. S-adenosylmethionine is the major methyl group donor for methylation of DNA, RNA, proteins, metabolites, or phospholipids (Mato *et al.*, 1997). Overexpression of a SAM

synthetase gene in *Aspergillus nidulans* impacted development and secondary metabolism (Gerke *et al.*, 2012). Given the wide variety of target substrates of methyltransferases that use SAM as a methyl group donor, it is currently impossible to identify such targets in *T. calospora*.

Another notable S- and N-containing compound was ergothioneine (Sheridan *et al.*, 2016), an amino acid occurring primarily in fungi and not detected in plants. Thus, it was possible to trace this compound in symbiotic protocorms, where it was highly induced compared to MYC or FLM. Ergothioneine exhibits powerful antioxidant properties, and biosynthetic deficiency in *Aspergillus fumigatus* mutants indicates a role for growth under elevated oxidative stress conditions (Sheridan *et al.*, 2016). Its accumulation in SYMB suggests that *T. calospora* is experiencing an oxidative environment and responds with the accumulation of antioxidants.

Chitin and chitin-related metabolites in symbiosis

Chitin is the main structural component of fungal cell walls (Bowman & Free, 2006) and contains N in the form of N-acetyl glucosamine residues, joined by β -(1,4) linkages. In addition to its structural role, chitin is a source of signaling molecules that regulate plant–microbe interactions (Sánchez-Vallet *et al.*, 2015). Chito-oligosaccharides with a degree of polymerization of six to eight are recognized by chitin-specific plant receptors, thus inducing plant defense responses against pathogenic fungi (Pusztahelyi, 2018). However, the chitin oligomers accumulated in SYMB protocorms were much smaller, with a degree of polymerization of two (chitobiose) and three (chitotriose). Chitin oligomers may originate from a biosynthetic process, such as the chitin-derived signaling molecules synthesized by bacterial and fungal plant mutualists to prepare their hosts for colonization (Sánchez-Vallet *et al.*, 2015). Alternatively, chitin oligomers can be released from a longer chitin polymer by fungal and plant chitinases. Most plant chitinases are endochitinases that cleave randomly at internal sites in the chitin polymer (Rathore & Gupta, 2015). By hydrolyzing the cell wall chitinous components of fungal pathogens, plant chitinases release chitin oligomers that trigger the plant defense responses (Fukamizo & Shinya, 2019). Although we do not have direct evidence of the origin of chitobiose and chitotriose in SYMB protocorms, transcriptomic data suggests that they are generated by the activity of plant chitinases. In fact, only one of the two *T. calospora* chitin synthase genes expressed in SYMB was slightly upregulated. Conversely, plant chitinases belonging to GH18 and GH19 families were strongly induced in SYMB, in agreement with previous observations showing increased chitinase expression in symbiotic protocorms (Zhao *et al.*, 2013; Perotto *et al.*, 2014). Although plants produce endochitinases in response to phytopathogenic attacks (Kumar *et al.*, 2018), a role for chitinases in root symbioses has already been reported for arbuscular mycorrhiza and nodule symbioses. In arbuscular mycorrhiza, the strong expression of plant chitinases in arbusculated cells, mainly belonging to GH family 18, may reduce the amount of chitin elicitors released by the wall of the symbiotic fungus (Kasprzewska, 2003; Hogekamp *et al.*,

2011; Grover, 2012). Interestingly, short oligomers of two to five N-acetyl glucosamine residues, similar to those found in SYMB, have been reported to actively promote AM colonization (Volpe *et al.*, 2020). Further studies are required to elucidate the involvement of *S. vomeracea* chitinases during OM symbiosis.

Chitosan, the deacetylated form of chitin, is rare in the cell walls of Basidiomycetes (Di Mario *et al.*, 2008). It was therefore intriguing to find a similar enrichment of chitin and chitosan oligomers in SYMB protocorms. Chitosan is produced through the activity of chitin deacetylase, and upregulation of three *T. calospora* chitin deacetylase genes in SYMB protocorms suggests that chitin deacetylation is turned on in symbiosis. Chitin deacetylation inactivates the elicitor activity of chitin oligomers by conversion to ligand-inactive chitosan, and it has been reported as a strategy of endophytic fungi and soil-borne pathogens to prevent chitin-triggered plant immunity (Cord-Landwehr *et al.*, 2016; Gao *et al.*, 2019). Chitin deacetylases are also regulated in ectomycorrhizal and arbuscular mycorrhizal fungi during their interaction with plants (Balestrini & Bonfante, 2014), suggesting a role during symbiosis establishment and functioning.

Current challenges of metabolomic studies

Using metabolomics, we demonstrated a rearrangement of the metabolome in OM and changes in compounds possibly related to structural, signaling, defense, and nutrient functions. However, our approach also showed some limitations. In contrast to transcriptomic analysis, where genes are species-specific, the same metabolite is often present in different organisms, hampering the analysis of mixed symbiotic samples. Also, since orchid seeds require different culture media to germinate aseptically and develop protocorms, a direct comparison between SYMB and ASYMB was difficult because some metabolic changes may originate from the different culture media. Nevertheless, this comparison usefully corroborated the changes seen in the fungal MYC/FLM comparison.

Another limitation was that several m.f. could not be annotated, resulting in a 'dark matter' that may contain crucial information. Overall, there is still a severe limitation in metabolite annotation in the study of nontargeted metabolomics: only ~2% of spectra are currently found in databases (da Silva *et al.*, 2015), that is, much less than for genomic annotations, which reach ~80%. Furthermore, metabolomics reports usually focus on model organisms, hampering analysis of nonmodel organisms such as *T. calospora* and *S. vomeracea* that are evolutionarily distant from organisms found in the database and, in the case of orchids, rich in as yet unknown secondary metabolites (Sut *et al.*, 2017). Although we used MetaCyc, the largest curated collection of metabolic pathways from all domains of life (Caspi *et al.*, 2018, 2019), 451 metabolites in the MYC/FLM comparison could not be identified, limiting our reconstruction of biochemical pathways. Nevertheless, we could estimate the elemental formulas of detected mass features. Using an ultra-high mass resolution and following the 'seven golden rules' (Kind & Fiehn, 2007), we were able to accurately measure the mass-to-charge ratios of the metabolome fingerprint and produce an excellent estimation of

the metabolite elemental formula with a high probability (Kim *et al.*, 2006, probability of 98%). Thus, we were able to classify many m.f. and overcome the constraints of actual databases.

In conclusion, we revealed profound changes in metabolite profiles – mainly a sharp adjustment of lipid metabolism in the external mycelium of *T. calospora* surrounding the symbiotic protocorms. Although further and more sensitive targeted analyses are needed to elucidate the significance of the metabolic changes observed in symbiosis, our study provides a more comprehensive understanding of the metabolic networks underlying orchid–fungus interactions.








Acknowledgements

The authors wish to acknowledge the anonymous referees and the editor for their valuable comments. The orchid mycorrhizal genome and transcriptomes were sequenced at the US Department of Energy Joint Genome Institute within the framework of the Mycorrhizal Genomics Initiative (CSP#305, Exploring the Genome Diversity of Mycorrhizal Fungi to Understand the Evolution and Functioning of Symbiosis in Woody Shrubs and Trees) coordinated by Francis Martin (INRA, Nancy, France). We thank Ronan le Gleut (ICB, Helmholtz Zentrum München, Germany) for statistical advice.

Author contributions

SP, RB and J-PS conceived and designed the research. AG, VF and BL conducted all wet lab experiments. AG, J-PS and MW conducted data analyses. AG, SP and RB wrote the manuscript. All authors read and approved the manuscript.

ORCID

Raffaella Balestrini  <https://orcid.org/0000-0001-7958-7681>
Valeria Fochi  <https://orcid.org/0000-0002-0757-8089>
Andrea Ghirardo  <https://orcid.org/0000-0003-1973-4007>
Birgit Lange  <https://orcid.org/0000-0002-2332-9154>
Silvia Perotto  <https://orcid.org/0000-0003-0121-1806>
Jörg-Peter Schnitzler  <https://orcid.org/0000-0002-9825-867X>
Michael Witting  <https://orcid.org/0000-0002-1462-4426>

References

- Aharoni A, Ric de Vos CH, Verhoeven HA, Maliepaard CA, Kruppa G, Bino R, Goodenowe DB. 2002. Nontargeted metabolome analysis by use of Fourier Transform Ion Cyclotron Mass Spectrometry. *OMICS: A Journal of Integrative Biology* 6: 217–234.
- Balestrini R, Bonfante P. 2014. Cell wall remodeling in mycorrhizal symbiosis: a way towards biotrophism. *Frontiers in Plant Science* 5: 1–10.
- Benjamini Y, Hochberg Y. 1995. Controlling the false discovery rate: a practical and powerful approach to multiple testing. *Journal of the Royal Statistical Society. Series B (Methodological)* 57: 289–300.
- Beyrle HF, Smith SE, Peterson RL, Franco CM. 1995. Colonization of *Orchis morio* protocorms by a mycorrhizal fungus: effects of nitrogen nutrition and glyphosate in modifying the responses. *Canadian Journal of Botany* 73: 1128–1140.

- Blunson NJ, Cockcroft S. 2020. Phosphatidylinositol synthesis at the endoplasmic reticulum. *Biochimica et Biophysica Acta - Molecular and Cell Biology of Lipids* 1865: 158471.
- Bowers WS, Hoch HC, Evans PH, Katayama M. 1986. Thallophtic allelopathy: isolation and identification of laetisarinic acid. *Science* 232: 105–106.
- Bowman SM, Free SJ. 2006. The structure and synthesis of the fungal cell wall. *BioEssays* 28: 799–808.
- Brodhun F, Feussner I. 2011. Oxylipins in fungi. *FEBS Journal* 278: 1047–1063.
- Cameron DD, Johnson I, Leake JR, Read DJ. 2007. Mycorrhizal acquisition of inorganic phosphorus by the green-leaved terrestrial orchid *Goodyera repens*. *Annals of Botany* 99: 831–834.
- Cameron DD, Johnson I, Read DJ, Leake JR. 2008. Giving and receiving: measuring the carbon cost of mycorrhizas in the green orchid, *Goodyera repens*. *New Phytologist* 180: 176–184.
- Cameron DD, Leake JR, Read DJ. 2006. Mutualistic mycorrhiza in orchids: evidence from plant–fungus carbon and nitrogen transfers in the green-leaved terrestrial orchid *Goodyera repens*. *New Phytologist* 171: 405–416.
- Carta G, Murru E, Banni S, Manca C. 2017. Palmitic acid: Physiological role, metabolism and nutritional implications. *Frontiers in Physiology* 8: 1–14.
- Casarrubia S, Martino E, Daghighi S, Kohler A, Morin E, Khouja H-R, Murat C, Barry KW, Lindquist EA, Martin FM *et al.* 2020. Modulation of plant and fungal gene expression upon Cd exposure and symbiosis in ericoid mycorrhizal *Vaccinium myrtillus*. *Frontiers in Microbiology* 11: 341.
- Caspi R, Billington R, Fulcher CA, Keseler IM, Kothari A, Krummenacker M, Latendresse M, Midford PE, Ong Q, Ong WK *et al.* 2018. The MetaCyc database of metabolic pathways and enzymes. *Nucleic Acids Research* 46: D633–D639.
- Caspi R, Billington R, Keseler IM, Kothari A, Krummenacker M, Midford PE, Ong WK, Paley S, Subhraveti P, Karp PD. 2019. The MetaCyc database of metabolic pathways and enzymes – a 2019 update. *Nucleic Acids Research* 48: D445–D453.
- Cassilly CD, Reynolds TB. 2018. PS, it's complicated: the roles of phosphatidylserine and phosphatidylethanolamine in the pathogenesis of *Candida albicans* and other microbial pathogens. *Journal of Fungi* 4: 28.
- Cavill R, Jennen D, Kleinjans J, Briedé JJ. 2016. Transcriptomic and metabolomic data integration. *Briefings in Bioinformatics* 17: 891–901.
- Chang DCN, Chou LC. 2007. Growth responses, enzyme activities, and component changes as influenced by *Rhizoctonia* orchid mycorrhiza on *Anoectochilus formosanus* Hayata. *Botanical Studies* 48: 445–451.
- Christensen SA, Kolomiets MV. 2011. The lipid language of plant–fungal interactions. *Fungal Genetics and Biology* 48: 4–14.
- Cord-Landwehr S, Melcher RLJ, Kolkenbrock S, Moerschbacher BM. 2016. A chitin deacetylase from the endophytic fungus *Pestalotiopsis* sp. efficiently inactivates the elicitor activity of chitin oligomers in rice cells. *Scientific Reports* 6: 1–11.
- Cowan AK. 2006. Phospholipids as plant growth regulators. *Plant Growth Regulation* 48: 97–109.
- Cumming BM, Chinta KC, Reddy VP, Steyn AJC. 2018. Role of ergothioneine in microbial physiology and pathogenesis. *Antioxidants and Redox Signaling* 28: 431–444.
- Dearnaley JDW, Cameron DD. 2017. Nitrogen transport in the orchid mycorrhizal symbiosis – further evidence for a mutualistic association. *New Phytologist* 213: 10–12.
- Der Wang K, Borrego EJ, Kenerley CM, Kolomiets MV. 2020. Oxylipins other than jasmonic acid are xylem-resident signals regulating systemic resistance induced by *Trichoderma virens* in maize. *The Plant Cell* 32: 166–185.
- Di Mario F, Rapanà P, Tomati U, Galli E. 2008. Chitin and chitosan from Basidiomycetes. *International Journal of Biological Macromolecules* 43: 8–12.
- Ebert B, Rautengarten C, McFarlane HE, Rupasinghe T, Zeng W, Ford K, Scheller HV, Bacic A, Roessner U, Persson S *et al.* 2018. A Golgi UDP-GlcNAc transporter delivers substrates for N-linked glycans and sphingolipids. *Nature Plants* 4: 792–801.
- Epstein S, Castillon GA, Qin Y, Riezman H. 2012. An essential function of sphingolipids in yeast cell division. *Molecular Microbiology* 84: 1018–1032.
- Ercole E, Adamo M, Rodda M, Gebauer G, Giralanda M, Perotto S. 2015a. Temporal variation in mycorrhizal diversity and carbon and nitrogen stable isotope abundance in the wintergreen meadow orchid *Anacamptis morio*. *New Phytologist* 205: 1308–1319.
- Ercole E, Rodda M, Giralanda M, Perotto S. 2015b. Establishment of a symbiotic *in vitro* system between a green meadow orchid and a *Rhizoctonia*-like fungus. *Bio-protocol* 5: 1–7.
- Fiehn O, Kopka J, Dörmann P, Altmann T, Trethewey RN, Willmitzer L. 2000. Metabolite profiling for plant functional genomics. *Nature Biotechnology* 18: 1157–1161.
- Fochi V, Chitarra W, Kohler A, Voyron S, Singan VR, Lindquist EA, Barry KW, Giralanda M, Grigoriev IV, Martin F *et al.* 2017a. Fungal and plant gene expression in the *Tulasnella calospora* – *Serapias vomeracea* symbiosis provides clues about nitrogen pathways in orchid mycorrhizas. *New Phytologist* 213: 365–379.
- Fochi V, Falla N, Giralanda M, Perotto S, Balestrini R. 2017b. Cell-specific expression of plant nutrient transporter genes in orchid mycorrhizae. *Plant Science* 263: 39–45.
- Fukamizo T, Shinya S. 2019. Chitin/Chitosan-active enzymes involved in plant–microbe interactions. In: Yang Q, Fukamizo T eds. *Targeting chitin-containing organisms. Advances in experimental medicine and biology*. Singapore: Springer, Vol. 1142, 253–272.
- Gao F, Sen Zhang B, Zhao JH, Huang JF, Jia PS, Wang S, Zhang J, Zhou JM, Guo HS. 2019. Deacetylation of chitin oligomers increases virulence in soil-borne fungal pathogens. *Nature Plants* 5: 1167–1176.
- Gerke J, Bayram Ö, Braus GH. 2012. Fungal S-adenosylmethionine synthetase and the control of development and secondary metabolism in *Aspergillus nidulans*. *Fungal Genetics and Biology* 49: 443–454.
- Ghirardo A, Heller W, Fladung M, Schnitzler J-P, Schroeder H. 2012. Function of defensive volatiles in pedunculate oak (*Quercus robur*) is tricked by the moth *Tortrix viridana*. *Plant, Cell & Environment* 35: 2192–2207.
- Ghirardo A, Sørensen HA, Petersen M, Jacobsen S, Søndergaard I. 2005. Early prediction of wheat quality: analysis during grain development using mass spectrometry and multivariate data analysis. *Rapid Communications in Mass Spectrometry* 19: 525–532.
- Ghirardo A, Xie J, Zheng X, Wang Y, Grote R, Block K, Wildt J, Mentel T, Kiendler-Scharr A, Hallquist M *et al.* 2016. Urban stress-induced biogenic VOC emissions impact secondary aerosol formation in Beijing. *Atmospheric Chemistry and Physics* 15: 2901–2920.
- Giralanda M, Segreto R, Cafasso D, Liebel HT, Rodda M, Ercole E, Cozzolino S, Gebauer G, Perotto S. 2011. Photosynthetic Mediterranean meadow orchids feature partial mycoheterotrophy and specific mycorrhizal associations I. *American Journal of Botany* 98: 1148–1163.
- Grover A. 2012. Plant chitinases: genetic diversity and physiological roles. *Critical Reviews in Plant Sciences* 31: 57–73.
- Hannun YA, Obeid LM. 2018. Sphingolipids and their metabolism in physiology and disease. *Nature Reviews Molecular Cell Biology* 19: 175–191.
- van der Heijden MGA, Martin FM, Selosse MA, Sanders IR. 2015. Mycorrhizal ecology and evolution: the past, the present, and the future. *New Phytologist* 205: 1406–1423.
- Hill EM, Robinson LA, Abdul-Sada A, Vanbergen AJ, Hodge A, Hartley SE. 2018. Arbuscular mycorrhizal fungi and plant chemical defence: effects of colonisation on aboveground and belowground metabolomes. *Journal of Chemical Ecology* 44: 198–208.
- Hogekamp C, Arndt D, Pereira PA, Becker JD, Hohnjec N, Küster H. 2011. Laser microdissection unravels cell-type-specific transcription in arbuscular mycorrhizal roots, including CAAT-Box transcription factor gene expression correlating with fungal contact and spread. *Plant Physiology* 157: 2023–2043.
- Hu W, Pan X, Abbas HMK, Li F, Dong W. 2017. Metabolites contributing to *Rhizoctonia solani* AG-1-IA maturation and sclerotial differentiation revealed by UPLC-QTOF-MS metabolomics. *PLoS ONE* 12: 1–16.
- Hua MD, Senthil Kumar R, Shyur L, Cheng Y-B, Tian Z, Oelmüller R, Yeh K-W. 2017. Metabolomic compounds identified in *Piriformospora indica*-colonized Chinese cabbage roots delineate symbiotic functions of the interaction. *Scientific Reports* 7: 9291.
- Kaling M, Kanawati B, Ghirardo A, Albert A, Winkler JB, Heller W, Barta C, Loreto F, Schmitt-Kopplin P, Schnitzler J-PP. 2015. UV-B mediated metabolic rearrangements in poplar revealed by non-targeted metabolomics. *Plant, Cell & Environment* 38: 892–904.
- Kasprzewska A. 2003. Plant chitinases - regulation and function. *Cellular and Molecular Biology Letters* 8: 809–824.

- Kay JG, Grinstein S. 2011. Sensing phosphatidylserine in cellular membranes. *Sensors* 11: 1744–1755.
- Kersten B, Ghirardo A, Schnitzler J, Kanawati B, Schmitt-Kopplin P, Fladung M, Schroeder H. 2013. Integrated transcriptomics and metabolomics decipher differences in the resistance of pedunculate oak to the herbivore *Tortrix viridana* L. *BMC Genomics* 14: 737.
- Keymer A, Pimprikar P, Wewer V, Huber C, Brands M, Bucerius SL, Delaux P, Klingl V, Wang TL, Eisenreich W. 2017. Lipid transfer from plants to arbuscular mycorrhiza fungi. *eLife* 6: e29107.
- Kim S, Rodgers RP, Marshall AG. 2006. Truly 'exact' mass: Elemental composition can be determined uniquely from molecular mass measurement at ~0.1 mDa accuracy for molecules up to ~500 Da. *International Journal of Mass Spectrometry* 251: 260–265.
- Kind T, Fiehn O. 2007. Seven Golden Rules for heuristic filtering of molecular formulas obtained by accurate mass spectrometry. *BMC Bioinformatics* 8: 1–20.
- Kluger B, Lehner S, Schuhmacher R. 2015. Metabolomics and secondary metabolite profiling of filamentous fungi. In: Zeilinger S, Martín J, García-Estrada C eds. *Biosynthesis and molecular genetics of fungal secondary metabolites, vol. 2. Fungal biology*. New York, NY, USA: Springer, 81–101.
- Kohler A, Böcker U, Shapaval V, Forsmark A, Andersson M, Warringer J, Martens H, Omholt SW, Blomberg A. 2015a. High-throughput biochemical fingerprinting of *Saccharomyces cerevisiae* by Fourier transform infrared spectroscopy. *PLoS ONE* 10: 1–22.
- Kohler A, Kuo A, Nagy LG, Morin E, Barry KW, Buscot F, Canbäck B, Choi C, Cichocki N, Clum A *et al.* 2015b. Convergent losses of decay mechanisms and rapid turnover of symbiosis genes in mycorrhizal mutualists. *Nature Genetics* 47: 410–415.
- Kuga Y, Sakamoto N, Yurimoto H. 2014. Stable isotope cellular imaging reveals that both live and degenerating fungal pelotons transfer carbon and nitrogen to orchid protocorms. *New Phytologist* 202: 594–605.
- Kumar M, Brar A, Yadav M, Chawade A, Vivekanand V, Pareek N. 2018. Chitinases—Potential candidates for enhanced plant resistance towards fungal pathogens. *Agriculture* 8: 88.
- Lallemant F, Martin-Magniette ML, Gilard F, Gakière B, Launay-Avon A, Delannoy É, Selosse MA. 2019. *In situ* transcriptomic and metabolomic study of the loss of photosynthesis in the leaves of mixotrophic plants exploiting fungi. *The Plant Journal* 98: 826–841.
- Laparre J, Malbreil M, Létisse F, Portais JC, Roux C, Bécard G, Puech-Pagès V. 2014. Combining metabolomics and gene expression analysis reveals that propionyl- and butyryl-carnitines are involved in late stages of arbuscular mycorrhizal symbiosis. *Molecular Plant* 7: 554–566.
- Leake JR. 1994. Tansley Review No. 69. The biology of myco-heterotrophic ('saprophytic') plants. *New Phytologist* 127: 171–216.
- Liu X-H, Liang S, Wei Y-Y, Zhu X-M, Li L, Ping-Ping Liu B, Zheng Q-X, Zhou H-N, Zhang Y, Mao L-J *et al.* 2019. Metabolomics analysis identifies sphingolipids as key function in *Magnaporthe oryzae*. *American Society for Microbiology* 10: 1–18.
- Majumder PL, Lahiri S. 1990. Lusianthrin and lusianthridin, two stilbenoids from the orchid *Lusia indivisa*. *Phytochemistry* 29: 621–624.
- Mato JM, Alvarez L, Ortiz P, Pajares MA. 1997. S-adenosylmethionine synthesis: molecular mechanisms and clinical implications. *Pharmacology and Therapeutics* 73: 265–280.
- Meijer HJG, Munnik T. 2003. Phospholipid-based signaling in plants. *Annual Review of Plant Biology* 54: 265–306.
- Mercx VSFT. 2013. *Mycobiotrophy: the biology of plants living on fungi*. New York, NY, USA: Springer.
- Miura C, Yamaguchi K, Miyahara R, Yamamoto T, Fuji M, Yagame T, Imaizumi-Anraku H, Yamato M, Shigenobu S, Kaminaka H. 2018. The mycoheterotrophic symbiosis between orchids and mycorrhizal fungi possesses major components shared with mutualistic plant-mycorrhizal symbioses. *Molecular Plant-Microbe Interactions* 31: 1032–1047.
- Obeid LM, Okamoto Y, Mao C. 2002. Yeast sphingolipids: Metabolism and biology. *Biochimica et Biophysica Acta - Molecular and Cell Biology of Lipids* 1585: 163–171.
- Oura T, Kajiwara S. 2010. *Candida albicans* sphingolipid C9-methyltransferase is involved in hyphal elongation. *Microbiology* 156: 1234–1243.
- Paley S, Parker K, Spaulding A, Tomb JF, O'Maille P, Karp PD. 2017. The omics dashboard for interactive exploration of gene-expression data. *Nucleic Acids Research* 45: 12113–12124.
- Pegg AE, Xiong H, Feith DJ, Shantz LM. 1998. S-adenosylmethionine decarboxylase: structure, function and regulation by polyamines. *Biochemical Society Transactions* 26: 580–586.
- Perotto S, Rodda M, Benetti A, Sillo F, Ercole E, Rodda M, Girlanda M, Murat C, Balestrini R. 2014. Gene expression in mycorrhizal orchid protocorms suggests a friendly plant-fungus relationship. *Planta* 239: 1337–1349.
- Peterson RL, Farquhar ML. 1994. Mycorrhizas: integrated development between roots and fungi. *Mycologia* 86: 311–326.
- Pusztahelyi T. 2018. Chitin and chitin-related compounds in plant-fungal interactions. *Mycology* 9: 189–201.
- R Core Team. 2019. *A language and environment for statistical computing*. Vienna, Austria: R Foundation for Statistical Computing. [WWW document] URL <https://www.R-project.org/>.
- Rasmussen HN. 1995. *Terrestrial orchids: from seed to mycotrophic plant*. Cambridge, UK: Cambridge University Press.
- Rathore AS, Gupta RD. 2015. Chitinases from bacteria to human: properties, applications, and future perspectives. *Enzyme Research* 2015: 1–9.
- Rivas-Ubach A, Liu Y, Bianchi TS, Tolić N, Jansson C, Paša-Tolić L. 2018. Moving beyond the van Krevelen diagram: a new stoichiometric approach for compound classification in organisms. *Analytical Chemistry* 90: 6152–6160.
- Rivero J, Álvarez D, Flors V, Azcón-Aguilar C, Pozo MJ. 2018. Root metabolic plasticity underlies functional diversity in mycorrhiza-enhanced stress tolerance in tomato. *New Phytologist* 220: 1322–1336.
- Rivero J, Gamir J, Aroca R, Pozo MJ, Flors V. 2015. Metabolic transition in mycorrhizal tomato roots. *Frontiers in Microbiology* 6: 598.
- Sánchez-Vallet A, Mesters JR, Thomma BPHJ. 2015. The battle for chitin recognition in plant-microbe interactions. *FEMS Microbiology Reviews* 39: 171–183.
- Schliemann W, Ammer C, Strack D. 2008. Metabolite profiling of mycorrhizal roots of *Medicago truncatula*. *Phytochemistry* 69: 112–146.
- Schumann U, Smith NA, Wang MB. 2013. A fast and efficient method for preparation of high-quality RNA from fungal mycelia. *BMC Research Notes* 6: 71.
- Sheridan KJ, Lechner BE, Keeffe GO, Keller MA, Werner ER, Lindner H, Jones GW, Haas H, Doyle S. 2016. Ergothioneine biosynthesis and functionality in the opportunistic fungal pathogen, *Aspergillus fumigatus*. *Scientific Reports* 6: 1–17.
- Shimura H, Matsuura M, Takada N, Koda Y. 2007. An antifungal compound involved in symbiotic germination of *Cypripedium macranthos* var. *rebunense* (Orchidaceae). *Phytochemistry* 68: 1442–1447.
- Sidorov RA, Zhukov AV, Pchelkin VP, Tsyndambaev VD. 2014. Palmitic acid in higher plant lipids. In: Lukas FP, ed. *Palmitic acid: occurrence, biochemistry and health effects*. Hauppauge, NY, USA: Nova Science, 124–144.
- Siebers M, Brands M, Wewer V, Duan Y, Hölzl G, Dörmann P. 2016. Lipids in plant-microbe interactions. *Biochimica et Biophysica Acta - Molecular and Cell Biology of Lipids* 1861: 1379–1395.
- da Silva RR, Dorrestein PC, Quinn RA. 2015. Illuminating the dark matter in metabolomics. *Proceedings of the National Academy of Sciences, USA* 112: 12549–12550.
- Singh A, Del Poeta M. 2016. Sphingolipidomics: an important mechanistic tool for studying fungal pathogens. *Frontiers in Microbiology* 7: 1–14.
- Smith S, Read D. 2008. *Mycorrhizal symbiosis*. Cambridge, UK: Academic Press.
- Suhre K, Schmitt-Kopplin P. 2008. MassTRIX: mass translator into pathways. *Nucleic Acids Research* 36: 481–484.
- Sut S, Maggi F, Dall'Acqua S. 2017. Bioactive secondary metabolites from orchids (Orchidaceae). *Chemistry and Biodiversity* 14: e1700172.
- Tschaplinski TJ, Plett JM, Engle NL, Deveau A, Cushman KC, Martin MZ, Doktycz MJ, Tuskan GA, Brun A, Kohler A *et al.* 2014. *Populus trichocarpa* and *Populus deltoides* exhibit different metabolomic responses to colonization by the symbiotic fungus *Laccaria bicolor*. *Molecular Plant-Microbe Interactions* 27: 546–556.
- Valentín-Berrios S, González-Velázquez W, Pérez-Sánchez L, González-Méndez R, Rodríguez-Del Valle N. 2009. Cytosolic phospholipase A: a member of the

- signalling pathway of a new G protein α subunit in *Sporothrix schenckii*. *BMC Microbiology* 9: 1–16.
- Van Van Waes JM, Debergh PC. 1986. *In vitro* germination of some Western European orchids. *Physiologia Plantarum* 67: 253–261.
- Vences-Guzmán MA, Geiger O, Sohlenkamp C. 2008. *Sinorhizobium meliloti* mutants deficient in phosphatidylserine decarboxylase accumulate phosphatidylserine and are strongly affected during symbiosis with alfalfa. *Journal of Bacteriology* 190: 6846–6856.
- Volpe V, Carotenuto G, Berzero C, Cagnina L, Puech-Pagès V, Genre A. 2020. Short chain chito-oligosaccharides promote arbuscular mycorrhizal colonization in *Medicago truncatula*. *Carbohydrate Polymers* 229: 115505.
- Wägele B, Witting M, Schmitt-Kopplin P, Suhre K. 2012. Masstrix reloaded: combined analysis and visualization of transcriptome and metabolome data. *PLoS ONE* 7: 1–5.
- Way D, Ghirardo A, Kanawati B, Esperschütz J, Monson RK, Jackson RB, Schmitt-Kopplin P, Schnitzler J-P. 2013. Increasing atmospheric CO₂ reduces metabolic and physiological differences between isoprene- and non-isoprene-emitting poplars. *The New phytologist* 200: 534–546.
- Yeh CM, Chung KM, Liang CK, Tsai WC. 2019. New insights into the symbiotic relationship between orchids and fungi. *Applied Sciences* 9: 1–14.
- Zhang N, Venkateshwaran M, Boersma M, Harms A, Howes-Podoll M, den Os D, Ané JM, Sussman MR. 2012. Metabolomic profiling reveals suppression of oxylipin biosynthesis during the early stages of legume–rhizobia symbiosis. *FEBS Letters* 586: 3150–3158.
- Zhao MM, Zhang G, Zhang DW, Hsiao YY, Guo SX. 2013. ESTs analysis reveals putative genes involved in symbiotic seed germination in *Dendrobium officinale*. *PLoS ONE* 8: e72705.

Supporting Information

Additional Supporting Information may be found online in the Supporting Information section at the end of the article.

Fig. S1 Van Krevelen diagrams.

Fig. S2 Cumulative changes in lipid biosynthesis.

Table S1 Metabolomic annotation.

Table S2 Statistical analysis of MSCC enrichment analysis.

Table S3 Gene expression in *Tulasnella calospora*.

Table S4 Gene expression in *Serapias vomeracea*.

Please note: Wiley Blackwell are not responsible for the content or functionality of any Supporting Information supplied by the authors. Any queries (other than missing material) should be directed to the *New Phytologist* Central Office.